IEEE/CSC & ESAS SUPERCONDUCTIVITY NEWS FORUM (global edition), January 2017 (Preview 1).
Preprint of ASC 2016 manuscript 3EPO2C-02 submitted to *IEEE Trans. Appl. Supercond.* for possible publication.
DOI: 10.1109/TASC.2016.2631840

Microwave Loss Measurements of Copper-Clad Superconducting Niobium Microstrip Resonators on Flexible Polyimide Substrates

Rujun Bai, George A. Hernandez, Yang Cao, John A. Sellers, Charles D. Ellis, *Member, IEEE,* David B. Tuckerman, *Fellow, IEEE,* and Michael C. Hamilton, *Senior Member, IEEE,*

***Abstract*—In this work, we investigated how different under- and capping layers on patterned Nb films impacted the rf losses of flexible thin-film superconducting microstrip transmission line resonators measured in a frequency range from 2-20 GHz. We studied how different thicknesses of Ti(10 and 50 nm) under-layer, used for adhesion, impacts conductor losses. We also studied Cu(20, 50, 100, and 200 nm) capping layers and how they affect conductor loss. These studies were carried out on 20 μm thick spin-on polyimide (PI-2611) thin films and characterized at various cryogenic temperatures between 1.2 K and 4.2 K. The results indicate normal-superconductor (Ti/Nb) and superconductor-normal (Nb/Cu) bilayer structures have increased surface resistance, which leads to an increase in microwave loss when compared to Nb-only signal traces. We quantified this additional loss by extracting resonator quality factors for weakly coupled resonators with various conductor stack-ups. Our experimental results can help inform decisions regarding material stack-ups when designing multi-conductor, multi-layer superconducting flexible cables intended for use with ultra-low temperature electronic systems.**

***Keywords*—microwave, conductor loss, superconducting proximity effect, polyimide.**

I. Introduction

In order to improve adhesion and enhance reliability, superconducting bilayer structures have been used [1]–[5]. When a normal thin-film metal and a superconducting thin-film metal are deposited on top of one another, proximity effects can affect the behavior of the bilayer structure. Depending on thickness, some or all of the normal metal layer can show superconductor-like behavior, e.g., zero dc resistance when it is below a transition temperature and the normal metal begins to exhibit a Ginzburg-Landau coherence length [6], [7]. This proximity effect can be beneficial, as it reduces the rf losses that would otherwise be caused by the presence of the normal metal. This work is aimed at providing experimental information regarding materials choices for conductor stack-ups that are candidates for use in high performance superconducting flexible cables with multiple conductor layers and multiple signal traces.

We gratefully acknowledge funding and technical guidance from Microsoft Research for this work.

R. Bai, G.A. Hernandez, Y. Cao, J.A. Sellers, C.D. Ellis and M.C. Hamilton are with the Department of Electrical and Computer Engineering, Auburn University, Auburn, AL, 36849 (e-mail: mch0021@auburn.edu)

D.B. Tuckerman is with Microsoft Research, Redmond, WA, 98052 (e-mail: v-datuck@microsoft.com)

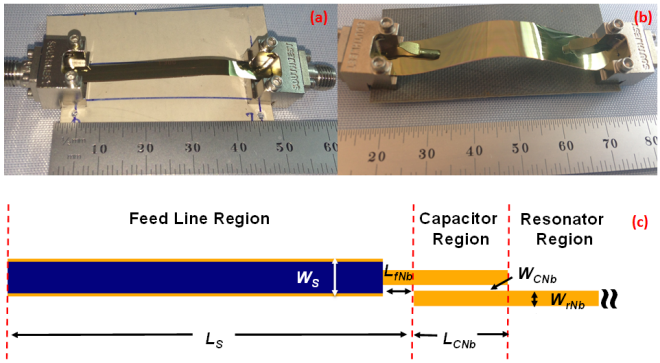

Fig. 1. (a) A ∼4.7 cm long flexible Ti/Nb microstrip resonator. (b) A ∼27.2 cm long (serpentine) flexible Nb/Cu resonator. (c) Design details of the launch and coupling structure of these resonators: L_s = 1200 μm, the width of the solder pad trace is 120 μm, L_c = 300 μm, W_{cgap} = 20 μm, W_{rMLine} = 47.6 μm

We first describe our investigation of Ti/Nb bilayers carried out using superconducting microstrip transmission line resonators. Titanium is a material commonly used as a thin-film under-layer to improve adhesion, and so we explored its use between polyimide and niobium. The pre-deposition of a Ti layer can also reduce the oxygen level in a deposition chamber by gettering and thereby improve the quality of the subsequently deposited Nb layer [2]. Although Ti is not normally a superconductor at 4.2 K, this type of bilayer (normal-superconductor) can exhibit proximity effects leading to the whole structure exhibiting superconductivity, particularly when the normal metal is thin and has good contact with the superconductor [8]. Even though this bilayer becomes superconducting, the thin normal metal layer is still expected to introduce additional rf losses since it is expected to be a poorer superconductor. In order to quantify the additional conductor loss caused by this thin Ti adhesion layer, we constructed a set of microstrip resonators with two different Ti thicknesses (10 nm and 50 nm) and measured the quality factors (Q) from 2 to 20 GHz.

We also investigated Nb/Cu bilayer metallization, since it can improve the mechanical reliability. Several groups have reported on the Ginzburg-Landau coherence length in a normal metal when in contact with a superconductor. Pambianchi, et al., reported the characterization results of Nb/Cu loss at 11.7

IEEE/CSC & ESAS SUPERCONDUCTIVITY NEWS FORUM (global edition), January 2017 (Preview 1).
Preprint of ASC 2016 manuscript 3EPO2C-02 submitted to *IEEE Trans. Appl. Supercond.* for possible publication.
DOI: 10.1109/TASC.2016.2631840

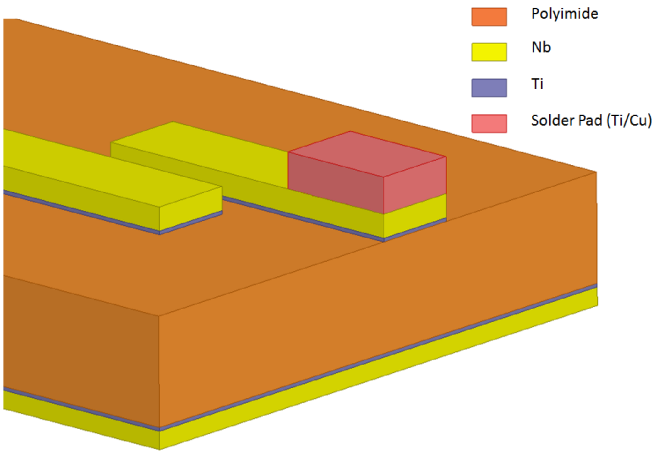

Fig. 2. Cross-section of a thin-film flexible superconducting Nb (250 nm thick) microstrip transmission line resonator with optional Ti under-layers (10 nm or 50 nm thick) to improve adhesion.

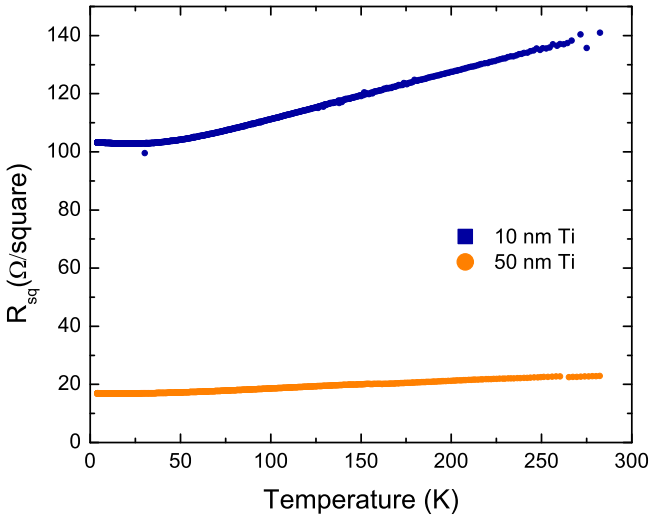

Fig. 3. Sheet resistance vs. temperature of 10 and 50 nm thick Ti films, measured on thermally oxidized silicon coupons using a pulse-tube cryostat.

GHz [9]; this single fixed frequency was a limitation of their measurement setup. Similar to our Ti/Nb studies, we characterized thin-film Nb/Cu structures using flexible microstrip resonators, providing rf loss data at multiple frequencies up to 11 GHz for varying copper thicknesses (20, 50, 100, and 200 nm) and varying temperatures.

II. Design and Fabrication

In this work, we used two different lengths of edge-coupled, half-wavelength microstrip resonators with the same launch structure and coupling gap design. A ∼4.7 cm long resonator design corresponding to a fundamental resonant frequency at approximately 2 GHz was used in the Ti/Nb study and is shown in Fig. 1a. The second design was a ∼27 cm long resonator with a fundamental resonant frequency of ∼350 MHz, shown in Fig. 1b; this design was used to study the impact of Cu cladding atop Nb. Design details of the solder pad and coupling structures are shown in Fig. 1c.

The polyimide film that was used in this work was PI-2611 from HD MicroSystems. Si "handle" wafers were prepared with an evaporated Cr/Al metallization layer, onto which the polyimide was spun on to produce a nominal cured thickness of 20 μm. Following curing of the polyimide layer, a conventional photolithography process was used to define signal traces and then solder pad structures that were used to interface to edge-launch SMA connectors. The samples were then released from the Si handle wafer following the process outlined by Metz et al. [10]. The ground plane was then deposited onto the back-side of the released (free-standing) films. A more detailed process flow description is provided in [11]. All Nb metallization was nominally 250 nm thick.

For the Ti/Nb studies, a schematic cross-section of the end of these resonators is shown in Fig. 2. Fig. 3 plots the sheet resistivity vs. temperature of the Ti layer (10 or 50 nm thick), as measured on thermally oxidized silicon "witness" coupons that experienced the same metallization deposition parameters as those used for depositing the Ti layers beneath the Nb layers on our polyimide films. Our thin-film polyimide resonators used the same thickness of Ti on both the signal and ground layers, which were e-beam deposited immediately prior to the Nb sputter-deposition.

For the Nb/Cu studies, we followed a fabrication flow that kept the Nb/Cu interface the same for all the samples. We sputter-deposited a 250-nm thick Nb film on four wafers, followed by electron-beam physical vapor deposition of a 20 nm Cu layer. Then, one wafer was removed from the deposition chamber and stored in a controlled N_2 environment. A second pump down of the chamber containing the three remaining wafers was performed, followed by a one minute ion-milling clean to remove any oxidized Cu. Next, a second Cu deposition was performed to deposit an additional 30 nm of Cu (50 nm total Cu). One wafer was again removed from the deposition chamber and stored. This procedure was was repeated, to yield wafers with 100 and 200 nm Cu layers. In this way, we obtained four wafers with the same Nb layer but different Cu layer thickness: 20, 50, 100, and 200 nm. The benefit of depositing the Cu metal this way was that all samples had identical Nb layers and identical Nb/Cu interfaces, thus ensuring that Cu thickness was the only variable between wafers. In order to prevent Cu from oxidation during later processing, we removed all four wafers from the N_2 storage and placed them back into the deposition chamber to receive a one-minute ion clean process, followed by deposition of a thin (10 nm) protective Au layer. Then, all four wafers underwent the same solder pad (under-bump metal (UBM) layer definition and deposition, film release process and ground-plane Nb deposition process. Furthermore, to reduce variations in the ground plane deposition, we sputter-deposited the Nb ground plane on all four released substrates during the same run.

Based on the theory of proximity effect, the thicker Cu coatings might cause some suppression of the Nb superconductivity. However, the measured critical temperatures of witness

DOI: 10.1109/TASC.2016.2631840

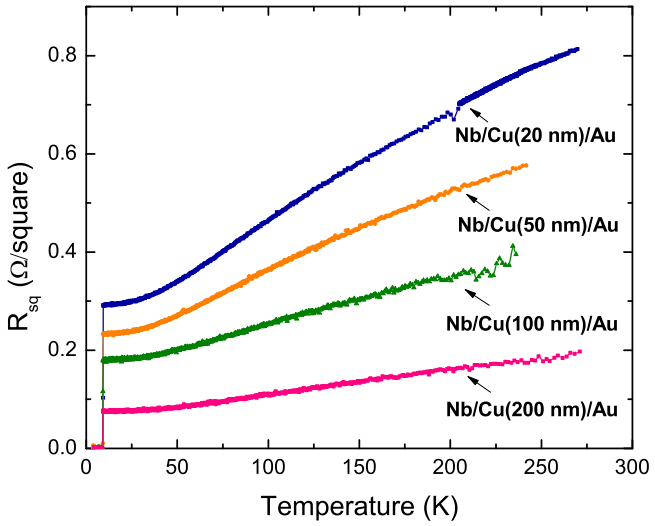

Fig. 4. Measured dc sheet resistance vs. temperature of Nb(250 nm)/Cu(20 nm, 50 nm, 100 nm or 200 nm)/Au(10 nm) films on SiO_2 witness die. All versions transitioned at $\sim$ 9.1 K.

SiO_2 samples from the Nb/Cu combinations, shown in Fig. 4, were all consistent at approximately 9.1 K.

III. Results and Discussion

We characterized the microwave performance of the different samples in a pulse-tube based cryostat capable of reaching a temperature as low as 1.2 K. In order to reduce the effect of humidity on the polyimide dielectric, we performed a dehydration bake in a vacuum oven at 90 °C for two hours immediately before loading samples into the cryostat. Our measurement temperature ranged from 4.2 K to 1.2 K, but we were only able to efficiently record a limited number of data points at 1.2 K (since this requires actively pumping on condensed He in the sample chamber). Fig. 5 shows S_{21} response of one of the resonators (Nb/Cu(20 nm)/Au) measured at 1.2 K.

A. Characterization of the impact of Ti adhesion layer on conductor losses

For the set of Nb resonators with titanium under-layers, we measured the quality factor Q at temperatures including 4.2, 3.6, 3.0, and 1.2 K. We plot $1/Q$ for various resonant frequencies in Fig. 6. Each of the Q-factor results is an average of 10 measurements, which reduces errors caused by temperature drift of the cryostat.

From Fig. 6, we can clearly see the sample with the thickest Ti(50 nm) under-layer shows the lowest Q value and therefore the highest surface resistance, while the sample with only Nb shows the highest Q value at all the measurement temperatures. These results indicate that the underlying Ti layer introduces additional loss and this loss increases with increase of Ti layer thickness. This additional loss is not only thickness dependent, but also temperature dependent. The conductor loss decreases when the measurement temperature is decreased. At 1.2 K, the Q values of all three samples are high and quite comparable,

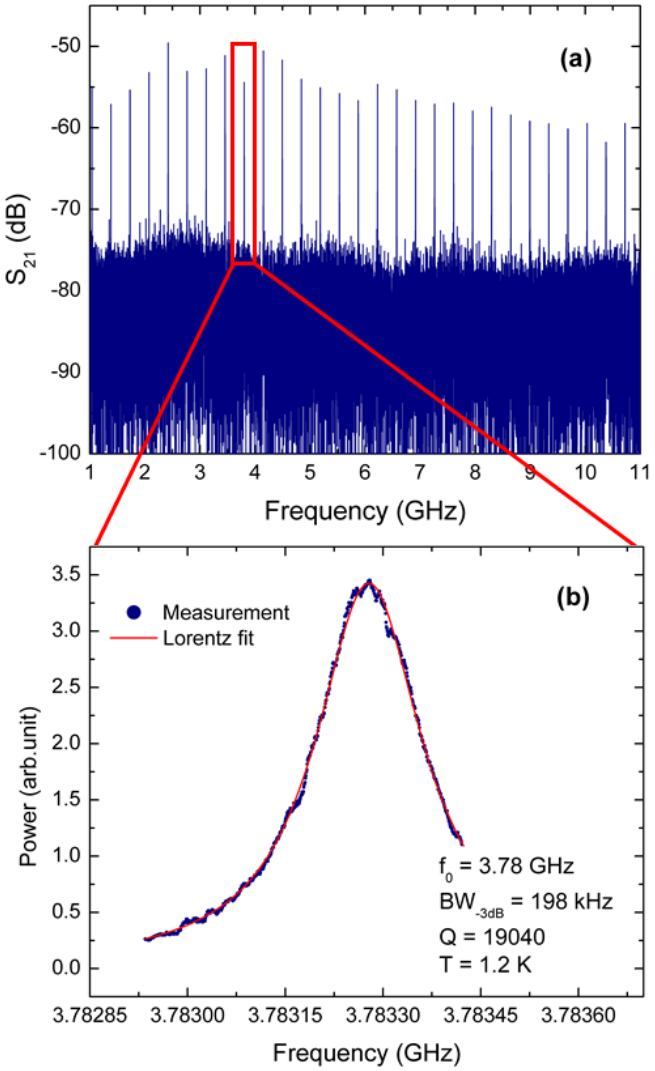

Fig. 5. S_{21} measurement results of a Nb/Cu(20 nm)/Au resonator measured at 1.2 K. (a) Broad frequency view and (b) zoomed-in view of one of the resonant harmonics along with Lorentz function fit used to calculate quality factor Q.

which indicates the Ti layer does not contribute significantly to the conductor loss at this temperature.

A possible explanation for this is that, at 1.2 K, the number of unpaired electrons in the Nb layer is reduced and leads to a more proximitized normal metal layer that exhibits a longer superconducting coherence length [12]. In this case, the overall number of unpaired electrons in this bilayer structure is lowest compared to other temperatures, resulting in lower conductor loss and higher Q. Also shown in Fig. 6 is a simulation result for lossless superconductors with lossless dielectric (i.e., exhibiting only coupling losses), from which we infer that the remaining losses at 1.2 K are primarily related to the non-zero loss tangent of the polyimide dielectric.

Preprint of ASC 2016 manuscript 3EPO2C-02 submitted to *IEEE Trans. Appl. Supercond.* for possible publication.
DOI: 10.1109/TASC.2016.2631840

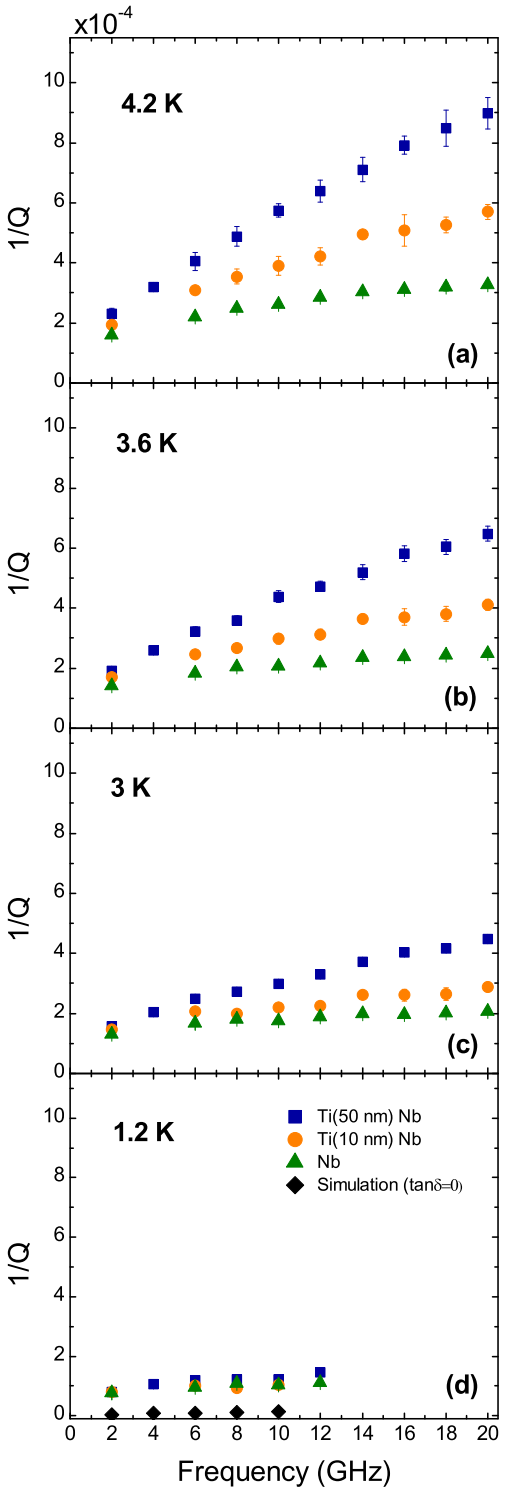

Fig. 6. $1/Q$ vs. resonant frequencies of Nb, Ti(10 nm)/Nb and Ti(50 nm)/Nb resonators at (a) 4.2 K, (b) 3.6 K, (c) 3 K, and (d) 1.2 K. Simulation results showing only coupling losses (i.e., for lossless superconductors and zero dielectric loss tangent) are also shown in (d).

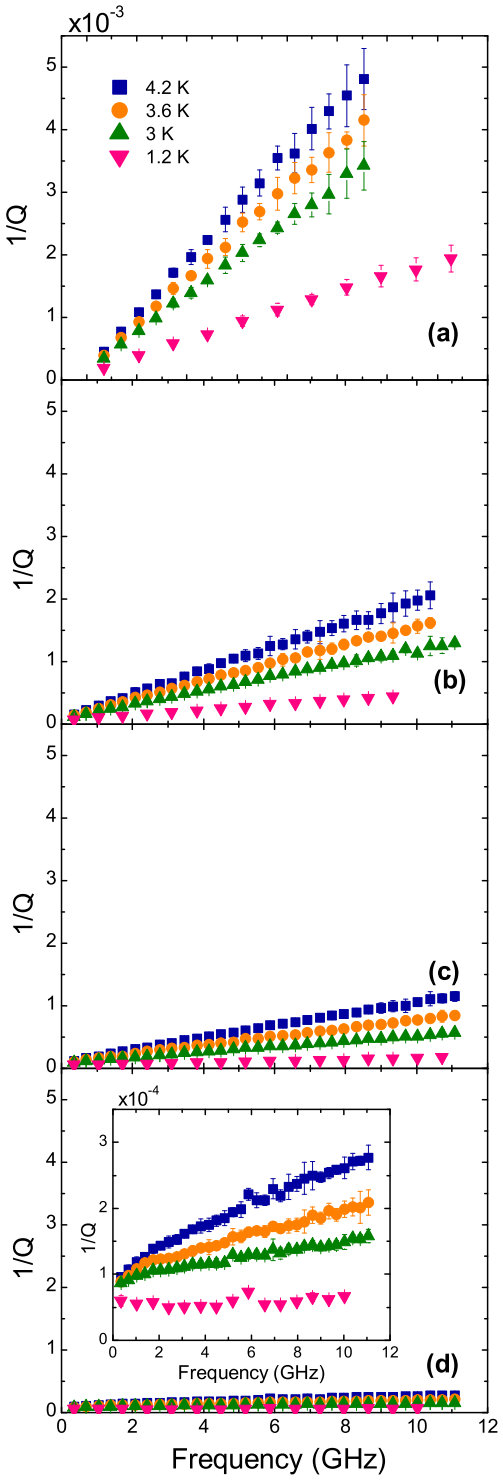

Fig. 7. $1/Q$ vs. resonant frequencies at various temperatures. Results for conductor stacks of: (a) Nb/Cu(200 nm)/Au, (b) Nb/Cu(100 nm)/Au, (c) Nb/Cu(50 nm)/Au and (d) Nb/Cu(20 nm)/Au. Inset plot is a close-up view of the $1/Q$ vs resonant frequency plot of Nb/Cu(20 nm)/Au.

Preprint of ASC 2016 manuscript 3EPO2C-02 submitted to *IEEE Trans. Appl. Supercond.* for possible publication.
DOI: 10.1109/TASC.2016.2631840

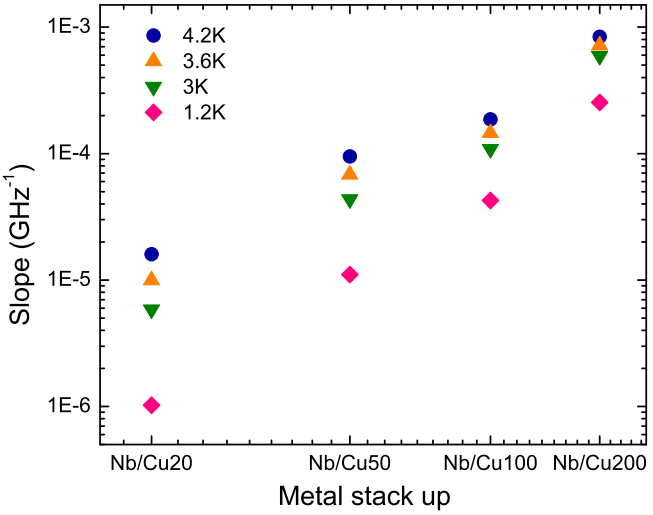

Fig. 8. Slope of $1/Q$ vs. resonance frequency plots of Nb/Cu(20, 50, 100, and 200 nm) resonators at 4.2, 3.6, 3, and 1.2 K.

B. Characterization of the impact of Cu cladding layer on conductor losses

Q-factor measurement results of the series of Nb/Cu resonators is shown in Fig. 7 at various measurement temperatures. We plot $1/Q$ vs. resonant frequency for each of the Cu thicknesses at 4.2 K, 3.6 K, 3 K and 1.2 K. In order to compare the different samples, we set the scale to be the same for these plots. To observe the temperature impact on the thinnest Cu sample clearly, we include an inset of re-scaled Nb/Cu(20 nm) resonator response at each of the temperatures. All of the Nb/Cu samples show a significant reduction of the conductor loss as measurement temperature is decreased. Furthermore, all of the Nb/Cu samples followed the rule of: $(1/Q) \times f$ = constant, similar to the Ti/Nb resonators, as would be expected from Bardeen-Cooper-Schrieffer (BCS) theory [13], [14].

Based on the ideas of proximity effect, the Cu region begins to show superconductivity as the measurement temperature decreases, leading to lower conductor loss [15]. Since all of these samples underwent the same initial deposition of Nb/Cu(20 nm), we yield four samples with the same superconductor (Nb) layer and the same superconductor-normal metal (Cu) interface. This allows us to quantify the proximity effect in these samples with different Cu thickness.

In Fig. 8, we summarized the slope information from the $1/Q$ vs. resonant frequency plots for each of the measurement temperatures. From Fig. 8, we note that these slopes exhibit an approximate square law relationship with the thickness of the Cu cladding layer. We can assume the depth of the proximity effect on all of these samples is similar at each of the measurement temperatures, since the Nb layer and Nb/Cu interface are identical. Then we can explain the slope difference arising directly from the different thickness of the Cu layers; the thicker Cu layers will have substantial non-proximitized conductor, contributing to the extra rf losses. [9].

In order to characterize the rf surface resistance (R_s) of the set of Nb/Cu(20, 50, 100, and 200 nm) resonators, we used

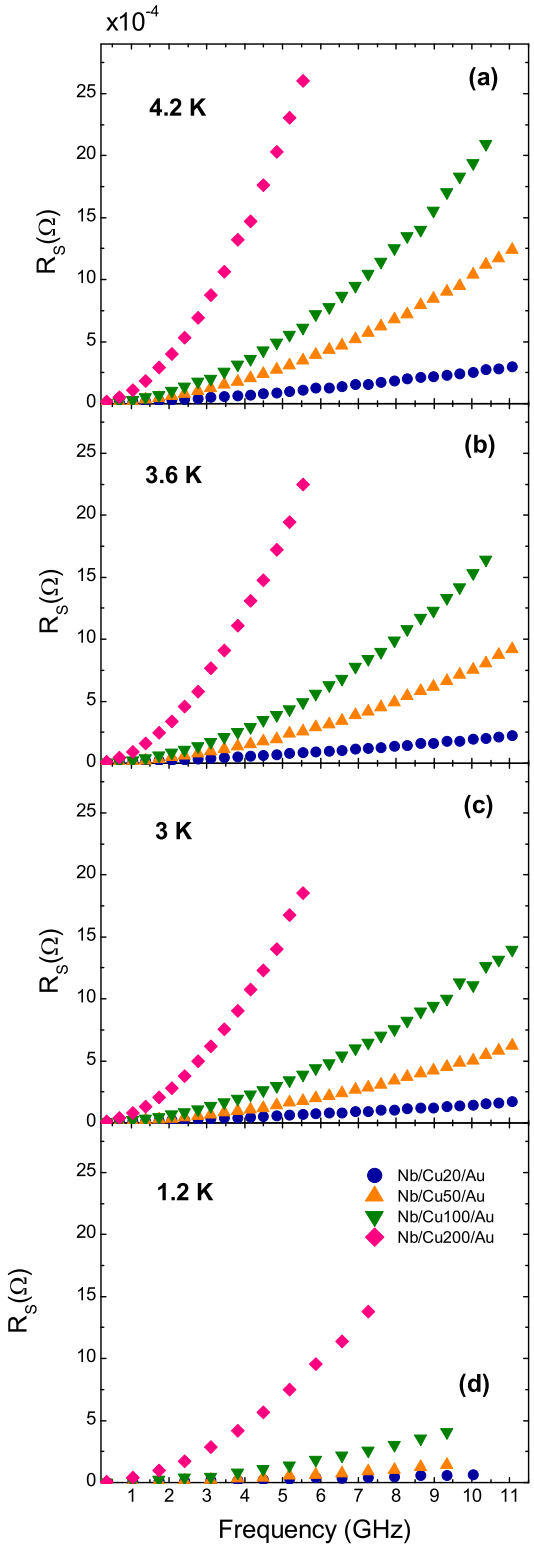

Fig. 9. Surface resistance of Nb/Cu(20 nm, 50 nm, 100 nm, 200 nm) resonators at (a) 4.2 K (b) 3.6 K (c) 3 K and (d) 1.2 K.

DOI: 10.1109/TASC.2016.2631840

the calculation methodology shown in the paper of Takemoto, et al. [16]. The results for different thicknesses of Cu on the Nb resonators at different temperatures are shown in Fig. 9. We can clearly see that the surface resistance is reduced as the temperature is decreased from 4.2 K to 1.2 K. Since the un-paired electrons contribute to the surface resistance, this reduction in the conductor loss can be attributed to a decrease of the quasi-particles in the Nb and increased thickness of the proximitized Cu layer. At 1.2 K, which is far below the Nb transition temperature (T_c ∼9.2 K), the un-paired electron density in the Nb layer is significantly lower, such that it can be ignored. Therefore the surface resistance difference should solely be due to the top Cu cladding layer. Since we have the same Nb layer and Nb/Cu interface, the coherence length in the Cu layer of all of the four samples at this temperature should be the same. Therefore, the additional surface resistance seen in the thicker Cu samples can be attributed to the non-proximitized electrons in the Cu layer.

IV. Conclusion

In this work, we investigated the impact of a Ti under-layer and Cu over-layer on Nb superconducting transmission line structures, and how these impact the microwave loss of superconducting resonators. We focused on thin Ti(10 and 50 nm) under-layer and different thickness of Cu(20, 50, 100, and 200 nm) as top cladding layers. All of these different metal stack-ups exhibited superconductivity at nearly the same transition temperature of ∼9 K. The quality factor measurement results showed that all the normal metal layers introduce additional conductor losses. These losses are reduced significantly with both decreasing normal conductor layer thickness and decreasing temperature, qualitatively consistent with how the proximity effect would be expected to behave. When the Cu layer is thin enough (below ∼50 nm), it does not introduce significant metal loss at ∼1.2 K. Results from these experiments may be useful for design and fabrication of robust and reliable flexible superconducting cables.

Acknowledgment

We thank AMNSTC staff for assistance with sample fabrication.

References

[1] H. Oguro, S. Awaji, K. Watanabe, M. Sugimoto, and H. Tsubouchi, "Prebending effect for mechanical and superconducting properties of Nb-rod-processed Cu–Nb internal-reinforced wires," *IEEE Transactions on Applied Superconductivity*, vol. 24, no. 3, pp. 1–4, 2014. [Online]. Available: http://dx.doi.org/10.1109/TASC.2013.2292507

[2] P. Kneisel, "Use of the titanium solid state gettering process for the improvement of the performance of superconducting rf cavities," *Journal of the Less Common Metals*, vol. 139, no. 1, pp. 179–188, 1988. [Online]. Available: http://dx.doi.org/10.1016/0022-5088(88)90340-2

[3] L. Thilly, F. Lecouturier, G. Coffe, and S. Askenazy, "Recent progress in the development of ultra high strength "continuous" Cu/Nb and Cu/Ta conductors for non-destructive pulsed fields higher than 80 T," *IEEE transactions on applied superconductivity*, vol. 12, no. 1, pp. 1181–1184, 2002. [Online]. Available: http://dx.doi.org/10.1109/TASC.2002.1018612

[4] A. Fartash, M. Grimsditch, E. E. Fullerton, and I. K. Schuller, "Breakdown of Poisson's effect in Nb/Cu superlattices," *Physical Review B*, vol. 47, no. 19, p. 12813, 1993. [Online]. Available: http://dx.doi.org/10.1103/PhysRevB.47.12813

[5] R. Bai, G. A. Hernandez, Y. Cao, J. A. Sellers, C. D. Ellis, D. B. Tuckerman, and M. C. Hamilton, "Cryogenic microwave characterization of kapton polyimide using superconducting resonators," in *2016 IEEE MTT-S International Microwave Symposium (IMS)*. IEEE, 2016, pp. 1–4.

[6] V. Kushnir, S. Prischepa, C. Cirillo, and C. Attanasio, "Proximity effect and interface transparency in Nb/Cu multilayers," *Journal of Applied Physics*, vol. 106, no. 11, 2009. [Online]. Available: http://dx.doi.org/10.1063/1.3267868

[7] L. Yu, N. Newman, and J. M. Rowell, "Measurement of the coherence length of sputtered Nb 0.62 Ti 0.38 N thin films," *IEEE transactions on applied superconductivity*, vol. 12, no. 2, pp. 1795–1798, 2002. [Online]. Available: http://dx.doi.org/10.1109/TASC.2002.1020339

[8] C. Kircher, "Superconducting proximity effect of Nb," *Physical Review*, vol. 168, no. 2, p. 437, 1968. [Online]. Available: http://dx.doi.org/10.1103/PhysRev.168.437

[9] M. Pambianchi, L. Chen, and S. M. Anlage, "Complex conductivity of proximity-superconducting Nb/Cu bilayers," *Physical Review B*, vol. 54, no. 5, p. 3508, 1996. [Online]. Available: http://dx.doi.org/10.1103/PhysRevB.54.3508

[10] S. Metz, A. Bertsch, and P. Renaud, "Partial release and detachment of microfabricated metal and polymer structures by anodic metal dissolution," *Microelectromechanical Systems, Journal of*, vol. 14, no. 2, pp. 383–391, 2005. [Online]. Available: http://dx.doi.org/10.1109/JMEMS.2004.839328

[11] D. B. Tuckerman, M. C. Hamilton, D. J. Reilly, R. Bai, G. A. Hernandez, J. M. Hornibrook, J. A. Sellers, and C. D. Ellis, "Flexible superconducting nb transmission lines on thin film polyimide for quantum computing applications," *Superconductor Science and Technology*, vol. 29, no. 8, p. 084007, 2016. [Online]. Available: http://dx.doi.org/10.1088/0953-2048/29/8/084007

[12] K. Matsumoto, S. Akita, Y. Tanaka, and O. Tsukamoto, "Proximity coupling effect in NbTi fine-multifilamentary superconducting composites," *Applied Physics Letters*, vol. 57, no. 8, pp. 816–818, 1990. [Online]. Available: http://dx.doi.org/10.1063/1.103429

[13] D. Hafner, M. Dressel, and M. Scheffler, "Surface-resistance measurements using superconducting stripline resonators," *Review of Scientific Instruments*, vol. 85, no. 1, p. 014702, 2014. [Online]. Available: http://dx.doi.org/10.1063/1.4856475

[14] D. Opie, H. Schone, M. Hein, G. Muller, H. Piel, D. Wehler, V. Folen, and S. Wolf, "A superconducting hydrogen maser resonator made from electrophoretic $YBa2Cu3O7\text{-}\delta$," *IEEE Transactions on Magnetics*, vol. 27, no. 2, pp. 2944–2947, 1991. [Online]. Available: http://dx.doi.org/10.1109/20.133826

[15] B. Strauss and R. Rose, "Strong proximity effects in Cu: Superconductivity of a fine Nb–Cu composite," *Journal of Applied Physics*, vol. 39, no. 3, pp. 1638–1644, 1968. [Online]. Available: http://dx.doi.org/10.1063/1.1656408

[16] J. H. Takemoto, C. M. Jackson, R. Hu, J. F. Burch, K. P. Daly, and R. W. Simon, "Microstrip resonators and filters using high-T_c superconducting thin films on $LaAlO_3$," *Magnetics, IEEE Transactions on*, vol. 27, no. 2, pp. 2549–2552, 1991. [Online]. Available: http://dx.doi.org/10.1109/20.133736